High sensitivity refractive index gas sensing enhanced by surface plasmon resonance with nano-cavity antenna array*

Zhao Hua-Jun(赵华君)†

Institute of Information Optoelectronics Technology and Application, Departments of Electronic and Electrical Engineering, Chongqing University of Arts and Sciences, Chongqing 402160, *China*

(Received 21 November 2011; revised manuscript received 13 January 2012)

The surface plasmon resonance gas sensor is presented for refractive index detection using nano-cavity antenna array. The gas sensor monitors the changes of the refractive index by measuring the spectral shift of the resonance dip, for modulating the wavelength of incident light. It is demonstrated that minute changes in the refractive index of a medium close to the surface of a metal film, owing to a shift in the resonance dip of the wavelength, can be detected. The average detection sensitivity is about 3200 nm/RIU (refractive index units), which is more than twice that of a metal grating-based gas sensor. The reflectivity of the surface plasmon resonance dip is only $\sim 0.03\%$, and the full widths at half maximum (FWHMs) of bandwidth of the angle and wavelength are $\sim 0.20^\circ$ and 4.71 nm, respectively.

Keywords: subwavelength structures, sensor, resonators, surface plasmons

PACS: 71.45.Lr, 87.19.lt, 73.20.Mf **DOI:** 10.1088/1674-1056/21/8/087104

1. Introduction

Surface plasmon polaritons (SPPs) are electromagnetic excitations propagating at the interface between a metal and a dielectric with permittivity of opposite signs, evanescently confined in the perpendicular direction.[1] Surface plasmon resonance (SPR) arises via the coupling of the electromagnetic fields to collective oscillation of the conduction electrons present at the interface of two media.[2] The SPR is highly sensitive to small changes in the local refractive index.[3] As a consequence, they are widely used in sensing applications.[4] Sensors based on SPR are highly dependent on the refractive index of the surrounding medium. The widely used methods of detecting SPR are based on attenuated total reflection (ATR) in a prism on which a thin metal film is coated.[5] In the method, transverse magnetic (TM) polarized light is incident on the metal film and the total internal reflection of the incident light is detected. Another widely used method is metallic diffraction grating for an SPR sensor.[6−8] The above methods involve reflection intensity versus incident angle (an angle-scan system); SPR has also been detected by modulating the wavelength of the incident light.[9,10] In addition, the reflections from different incident angles are collected simultaneously with a linear diode array or charge coupled device (CCD).[11]

An SPR curve can be characterized by three main parameters: the position of the dip, the peak height at the dip, and the width of the resonance dip. The position of the minimum is the quantity that is most sensitive to the real part of the refractive index of the adjacent medium, and therefore this quantity is usually used for the purpose of sensing.[12] For sensor applications, the refractive index change of a thin layer in contact with the metal surface of the sensor is monitored by measuring the spectral shift of the resonance dip.[13] Although both angular and wavelength modulations have been used in SPR applications, we use the wavelength modulation throughout this paper. To improve the resolution of the SPR sensor for a specific SPR configuration, it is desirable to reduce the width of the resonance feature, thereby reducing the uncertainty of the position of the resonance. Another possible route is to increase the sensitivity of the sensor. In our previous work, it is shown that the use of SPR technology can greatly enhance the local elec-

*Project supported by the Natural Science Foundation of Chongqing Science and Technology Program, China (Grant No. CSTC, 2010BB2352) and the Fund of Chongqing Education Committee (Grant No. KJ121224).

†Corresponding author. E-mail: zhaohjcu@163.com

© 2012 Chinese Physical Society and IOP Publishing Ltd

tromagnetic field by coupling the incident light wave into the nano-cavity antenna array.[14] In the present work, we design theoretically a novel refractive index sensor for gas with high sensitivity enhanced by SPR using the nano-cavity antenna array, in which a metallic grating is coated on a dielectric spacer atop an opaque metal film. In the periodic metallic nanostrips we employ a metallic grating that is introduced to convert incident light into SPP modes. All the results are calculated by the rigorous coupled wave analysis (RCWA) method.[15,16] A perfectly matched layer (PML) is used to avoid artificial reflections from the boundaries of the studied domain and the validity is confirmed by comparing the results for the structures studied in Refs. [17] and [18].

2. Gas sensor setup and principles

Figure 1 shows the SPR refractive index gas sensing system and the three-dimensional (3D) schematic diagram for the nano-cavity antennas formed by the metallic rectangular nanostrip array (with period Λ, width w, thickness h) over a metal film (with a distance of t). The filling ratio of the metallic nanostrip is $f = w/\Lambda$. Both the film and the nanostrips are made of silver, whose frequency-dependent permittivity functions are obtained from the tabulated data in Ref. [19]. In practice, the silver film, whose thickness is greater than the radiation penetration depth, can be deposited on a substrate of fused silica.

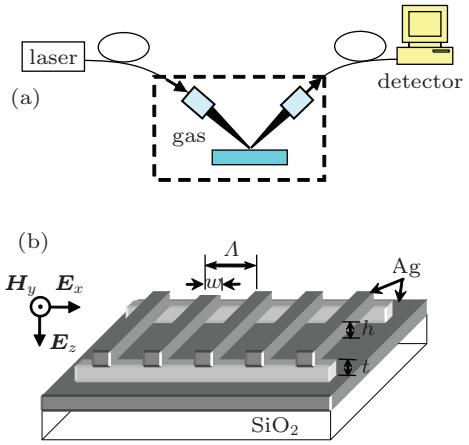


Fig. 1. (colour online) Diagram of (a) the system and (b) the 3D schematic plot of the refractive index sensor for the nano-cavity antenna array over a metal film deposited on a substrate of fused silica.

A TM polarized electromagnetic wave (the magnetic field is perpendicular to the x–z plane) incident at an incidence angle θ focuses on the metallic nanostrip array. If the wave vector of the incident wave matches with the plasmon wave vector, the SPR will be excited. The SPR manifests itself as a dip in the angular dependence of the intensity of the reflected light because the energy of the light beam is used to excite surface plasmons, which quickly decay with the conversion of their energy into heat during their propagation.[20] The array of metal strips provides a phase-matching condition for exciting SPPs, which transforms the incident light into the gas interlayer between the metallic nanostrip and the metal film. When the SPR has been excited, alternate positive/negative charges on the metallic rectangular nanostrip arrays are produced. Furthermore, the incident plane wave is converted into a strong localized surface plasmon wave (SPW) in the gas interlayer, which can evidently reduce the width of the resonance dip and also the peak height at the minimum, thereby increasing the sensitivity of the sensor.

3. Numerical simulation

The diffraction at a metallic diffraction grating provides additional momentum to compensate the wave vector mismatch between the incident wave and SPW. The matched condition of the wave vector is expressed as

$$\pm k_{\rm sp} = k\sqrt{\varepsilon_{\rm g}}\sin\theta_{\rm spr} + m\frac{2\pi}{\Lambda}, \tag{1}$$

where $k_{\rm sp} = k\sqrt{\varepsilon_{\rm m}\varepsilon_{\rm g}/(\varepsilon_{\rm m}+\varepsilon_{\rm g})}$, $k = 2\pi/\lambda$, $\theta_{\rm spr}$ is the resonant angle of incidence, $\varepsilon_{\rm m}$ is the permittivity of Ag, $\varepsilon_{\rm g}$ is the permittivity of the analysis gas which is in contact with the surface of the metal nanostrip, m is an integer representing the diffraction order, and Λ is the period of the grating. According to Eq. (1), we can deduce the SPR wavelength as

$$\lambda = \frac{\Lambda}{m}\left[\pm\sqrt{\frac{\varepsilon_{\rm m}n_{\rm g}^2}{\varepsilon_{\rm m}+n_{\rm g}^2}} - n_{\rm g}\sin\theta_{\rm spr}\right]. \tag{2}$$

Equation (2) shows the refractive index $n_{\rm g}$ as a function of resonant wavelength. It is easy to deduce the derivation of $\mathrm{d}\lambda/\mathrm{d}n_{\rm g}$ from Eq. (2), which indicates the sensitivity of the metallic grating gas sensor, as

$$\begin{aligned} G_{\rm s} &= \left|\frac{\mathrm{d}\lambda}{\mathrm{d}n_{\rm g}}\right| \\ &= \left|-\frac{\lambda}{n_{\rm g}} \pm \frac{\Lambda}{m}\left(\left(\frac{\varepsilon_{\rm m}}{\varepsilon_{\rm m}+n_{\rm g}^2}\right)^{3/2} - \sqrt{\frac{\varepsilon_{\rm m}}{\varepsilon_{\rm m}+n_{\rm g}^2}}\right)\right| \\ &\cong \frac{\lambda}{n_{\rm g}}. \end{aligned} \tag{3}$$

From Eq. (3) it follows that the sensitivity of the SPR refractive index sensors based on metallic grating using wavelength modulation increases with the wavelength increasing. The period of the grating and other parameters are less sensitive. The sensitivity of the sensor is easily obtained from Eq. (3). As an example, the sensitivity is ~ 1549.6 nm/RIU with incident wavelength 1550 nm, under the assumption of the hydrogen gas ($n_g = 1.000132$).

In order to increase the sensitivity of the refractive index gas sensor, we use a nano-cavity antenna array to enhance the local electromagnetic field. Figure 2 shows the refractive efficiency cures for the metallic grating (insert, Fig. 2(a)) and the nano-cavity antenna array (insert, Fig. 2(b)) SPR refractive index sensor with the same parameters (i.e. $\lambda = 1550$ nm, $\Lambda = 1400$ nm, $f = 0.5$, $h = 20$ nm, $\theta_{spr} = 5.55°$, and $n_g = 1.000132$) using the RCWA method. Note that the interval between the metallic rectangular nanostrip array and the metal film is $t = 100$ nm. Figure 2 shows that the metallic grating and the nano-cavity antenna array have a dip located at ~ 1550 nm wavelength for excited SPR. The resonance peak dip reflectivity is ~ 0.03 % for the nano-cavity antenna array, while the metallic grating reflection rate is about 56%. The wavelength resolution is ~ 3200 nm/RIU for the nano-cavity antenna array SPR sensor, which is twice the wavelength resolution of the metallic grating SPR refractive index sensor ($\sim$ 1500 nm/RIU). Figure 3 shows the sensitivity of the nano-cavity antenna array SPR sensor (solid line) and metallic grating SPR sensor (dotted line) using the wavelength interrogation as a function of the gas refractive index for $\Lambda = 1400$ nm, $f = 0.5$, $h = 20$ nm, $\theta_{spr} = 5.55°$, $t = 100$ nm, and $n_g = 1.000132$.

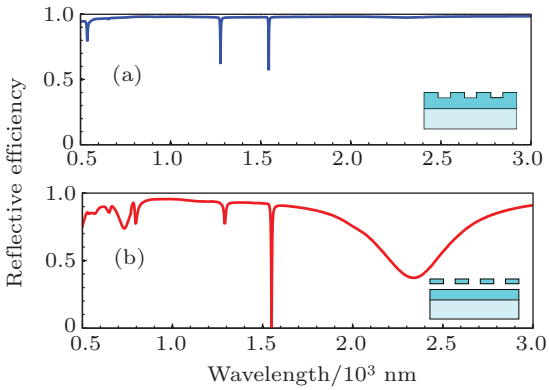


Fig. 2. (colour online) Refractive efficiency and the incident wavelength for (a) metallic grating and (b) nano-cavity antenna array SPR refractive index sensor. Inserts show the diagrams of (a) the metallic grating and (b) nano-cavity antenna array for $\lambda = 1550$ nm, $\Lambda = 1400$ nm, $f = 0.5$, $h = 20$ nm, $\theta_{spr} = 5.55°$, and $n_g = 1.000132$. The interval between the metallic rectangular nanostrip array and the metal film is $t = 100$ nm for the nano-cavity antenna array SPR refractive index sensor.

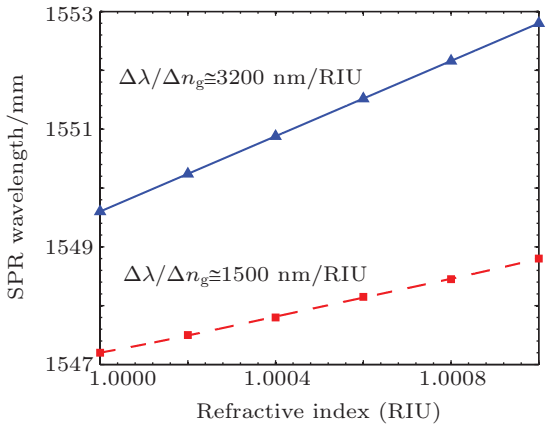


Fig. 3. (colour online) Dip positions (sensitivities) of the SPR wavelength for the nano-cavity antenna array SPR sensor (solid line) and the metallic grating SPR sensor (dotted line) using the wavelength interrogation each as a function of the gas refractive index for $\Lambda = 1400$ nm, $f = 0.5$, $h = 20$ nm, $\theta_{spr} = 5.55°$, $t = 100$ nm, and $n_g = 1.000132$.

Table 1. Performances of the refractive index SPR gas sensor with nano-cavity antenna array for different structure parameters for f= 0.5, h= 20 nm, and $n_g = 1.000132$.

Λ/nm	t/nm	θ_{spr}/(°)	Resonance peak reflectivity/%	FWHM/(°)	FWHM/nm	Wavelength resolution/(nm/RIU)
1500	200	1.29	0.36	0.19	4.75	2700
1400	100	5.55	0.03	0.20	4.71	3200
1300	70	10.51	0.17	0.21	4.72	3000
1200	50	16.40	0.20	0.22	4.29	3000
1100	30	23.58	0.26	0.25	3.99	3050

Using the RCWA method, the performances of the nano-cavity antenna array refractive index gas sensor are calculated with different periods, i.e., Λ = 1500 nm, 1400 nm, 1300 nm, 1200 nm, and 1100 nm for $f = 0.5$, $h = 20$ nm, and $n_g = 1.000132$ as shown in Table 1. The periods of the metallic strip are greater than 773 nm and less than 1541 nm (i.e. 773 nm< Λ <1541 nm) from Eq. (2). As the metallic strip period increases, the resonant angle will reduce. In order to diminish the peak height to the minimum and depress the width of the resonance dip, the distance between the metallic strip and the metal film needs to decrease as the strip period reduces (shows in Table 1), while the changes of the period of the metallic rectangular nanostrip array have less effect on sensing performances. As an example, when the period is 1400 nm, the wavelength resolution is $\sim$ 3200 nm/RIU, the SPR resonance peak reflectivity (i.e. the resonance dip) is only about 0.03%, the FWHMs of bandwidth of the angle and wavelength are only about 0.20° and 4.71 nm, respectively.

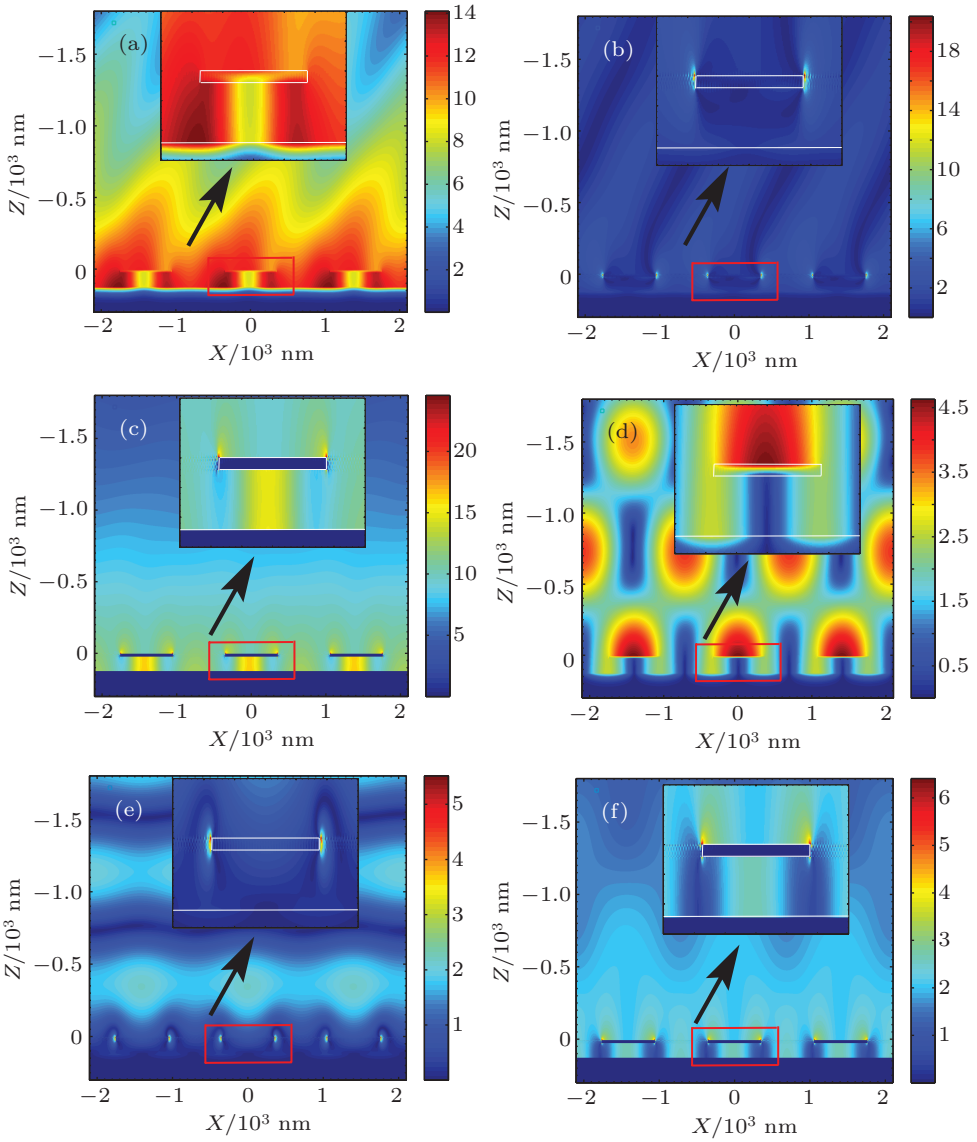


Fig. 4. (colour online) Distributions of the $|\boldsymbol{H}_y|$, $|\boldsymbol{E}_x|$, and $|\boldsymbol{E}_z|$ for exciting the SPR with (a) $|\boldsymbol{H}_y|$, $\lambda_0 = 1550$ nm; (b) $|\boldsymbol{E}_x|$, $\lambda_0 = 1550$ nm; (c) $|\boldsymbol{E}_z|$, $\lambda_0 = 1550$ nm, and not exciting the SPR with (d) $|\boldsymbol{H}_y|$, $\lambda_0 = 1540$ nm; (e) $|\boldsymbol{E}_x|$, $\lambda_0 = 1540$ nm; (f) $|\boldsymbol{E}_z|$, $\lambda_0 = 1540$ nm for $\Lambda = 1400$ nm, $f = 0.5$, $h = 20$ nm, $t = 100$ nm, $\theta_{spr} = 5.55°$, and $n_g = 1.000132$.

Figure 4 shows computed plots of $\boldsymbol{H}_y$, $\boldsymbol{E}_x$, and $\boldsymbol{E}_z$ for a nano-cavity antenna array for exciting the SPR ($\lambda_0 = 1550$ nm) and not exciting the SPR ($\lambda_0 = 1540$ nm) with $\Lambda = 1400$ nm, $f = 0.5$, $h = 20$ nm, $t = 100$ nm, $\theta_{spr} = 5.55°$, and $n_g = 1.000132$. If the incident light and the period of the nanocavity

antenna array wave vector are matched, SPR can be excited, and the incident wave couples into the gas interlayer as shown in Figs. 4(a)–4(c), where the incident wavelength is 1550 nm for $\Lambda = 1400$ nm, $f = 0.5$, $h = 20$ nm, $t = 100$ nm, $\theta = 5.55°$, and $n_g = 1.000132$. It shows that the electromagnetic field components are significantly enhanced between the metallic strip and the metal film. When the wave vector of the incident wave does not match with the plasmon wave vector, the SPR cannot be excited. The reflected H_y and E_x interfere with the corresponding incident fields to produce standing waves above the top surface as shown in Figs. 4(d) and 4(e). There are also a few electric fields below the metallic nanostrips shown in Fig. 4(f).

The refractive index SPR sensor is designed with fixed angle by measuring the changes of the wavelength resonance dip to determine the refractive index of the detection gas. Figure 5 shows the SPR spectra calculated using the RCWA method for $\Lambda = 1400$ nm, $f = 0.5$ nm, $h = 20$ nm, $t = 100$ nm, and $\theta_{spr} = 5.55°$. It shows that the shift of the wavelength resonance dip is linearly proportional to the change of the refractive index. In this present application, it is the intensity distribution due to an SPR wavelength shift rather than physical movement of the laser beam that is measured. When the gas refractive index difference $\Delta n_g = 0.001$ and the spectral shift of ~ 3.2 nm, the average detection sensitivity is 3200 nm/RIU. So the nano-cavity antenna array SPR gas sensor for refractive index inspected by modulating the wavelength of incident light has a high resolution.

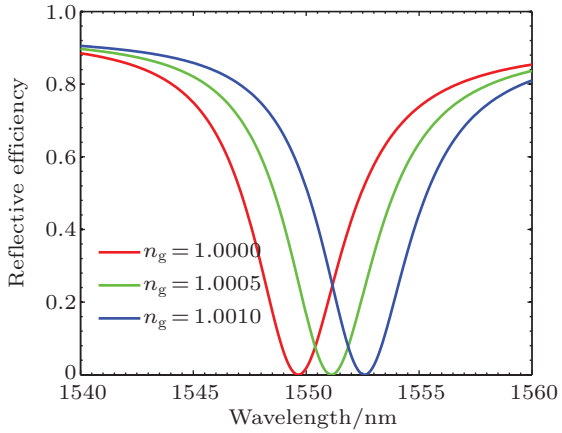


Fig. 5. (colour online) Resonance wavelength curves of the nano-cavity antenna array refractive index SPR gas sensor for $\Lambda = 1400$ nm, $f = 0.5$, $h = 20$ nm, $t = 100$ nm, and $\theta_{spr} = 5.55°$.

4. Conclusion

A theoretical investigation of the surface plasmon resonance gas sensor for refractive index detection is presented. The measuring procedure makes use of the modulation of the incident wavelength and monitors the changes of the refractive index by measuring the spectral shift of the resonance dip. A sensitivity of the SPR wavelength of ~ 3200 nm/RIU can be obtained, which is more than twice that of the metal grating-based gas sensor. The SPR resonance peak reflectivity is only about 0.03%, the FWHMs of bandwidth of the angle and wavelength are only $\sim 0.20°$ and ~ 4.71 nm, respectively.

References

[1] Maier S A 2007 *Plasmonics: Fundamentals and Applications* (Berline: Springer)
[2] Liedberg B, Nylander C and Lundstrom I 1983 *Sensors and Actuators* **4** 299
[3] Huang Q, Zhang X D, Zhang H, Xiong S Z, Geng W D, Geng X H and Zhao Y 2010 *Chin. Phys.* B **19** 047304
[4] Hao P, Wu Y H and Zhang P 2010 *Acta Phys. Sin.* **59** 6532 (in Chinese)
[5] Kretschmann E 1971 *Z. Phys.* **241** 313
[6] Roh S, Chung T and Lee B 2011 *Sensors* **11** 1565
[7] Hu C K and Liu D M 2010 *Mod. Appl. Sci.* **4** 8
[8] Cullen D C, Brown R G W and Lowe C R 1988 *Biosensors* **3** 211
[9] Lin K Q, Lu Y H, Chen J X, Zheng R S, Wang P and Ming H 2008 *Opt. Express* **16** 18599
[10] Caruso F, Jory M J, Bradberry G W, Sambles J R and Furlong D N 1998 *J. Appl. Phys.* **83** 1023
[11] Tao N, Boussaad S, Huang W, Arechabaleta R and Agnese J D 1999 *Rev. Sci. Instrum.* **70** 4656
[12] Nenninger G G, Tobiska P, Homola J and Yee S S 2001 *Actuators* B **74** 145
[13] Kolomenskii A, Gershon P D and Schuessler H A 1997 *Appl. Opt.* **36** 6539
[14] Zhao H J and Yuan D R 2010 *Chin. Opt. Lett.* **8** 1117
[15] Moharam M G, Grann E B, Pommet D A and Gaylord T K 1995 *J. Opt. Soc. Am.* A **12** 1068
[16] Li L F 1996 *J. Opt. Soc. Am.* A **13** 1870
[17] Lee J, Wang L P and Zhang Z M 2008 *Opt. Express* **16** 11328
[18] Cui Y X and He S L 2009 *Opt. Lett.* **34** 16
[19] Palik E D 1998 *Handbook of Optical Constants of Solids* (London: Academic Press)
[20] Inagaki T, Kagam K and Arakawa E T 1981 *Phys. Rev.* B **24** 3644